Int. J. Electrochem. Sci., 17 **(2022)** Article Number: 221254, doi: 10.20964/2022.12.54

International Journal of
ELECTROCHEMICAL
SCIENCE
www.electrochemsci.org

Corrosion Behavior of Aluminum in some Short-chain Carboxylic Acid solutions as a Simulant for Cooling Water in HVDC Transmission

Zhen Wang[1,2], Yanshen Zou[1,2], Kai Xiao[1,2], Youping Fan[3,], Shengping Wang[4,*]*

[1] Maintenance & Test Center, Extra High Voltage Power Transmission Company, China Southern Power Grid, Guangzhou 510620, China
[2] Joint Laboratory for Safe Operation of DC Transmission equipment and Submarine Cables, China Southern Power Grid, Guangzhou 510620, China
[3] School of Electrical Engineering and Automation, Wuhan University, Wuhan 430072, China
[4] Faculty of Material Science and Chemistry, China University of Geosciences, Wuhan 430074, China
[*]E-mail: ypfan@whu.edu.cn, spwang@cug.edu.cn

Received: 20 October 2022 / *Accepted:* 19 November 2022 / *Published:* 30 November 2022

The corrosion law of Al in various acidic solutions at 25 °C was determined in this study. The pH of 0.1 mM solutions of different weak acids was measured by a pH meter. Electrochemical tests were carried out using the polarization curve method and EIS. The activation energy of Al corrosion in different weakly acidic solutions was calculated by thermodynamic analysis. The results showed that the Al corrosion resistance was lowest in the formic acid solution and highest in the n-butyric acid solution. That is, Al in the n-butyric acid solution exhibited the lowest corrosion current density, the largest charge transfer impedance and the highest corrosion activation energy. The corrosion products of Al mainly exist in the form of $Al(OH)_3$ over a pH range between 3.7 and 4.7. The large anions in solution inhibit the ionization of weak acids and adsorb on the Al surface, thus inhibiting Al corrosion. The elucidation of the effect of anions on Al corrosion provides insight into the corrosion law of Al and a theoretical basis for identifying effective corrosion inhibitors.

Keywords: aluminum, corrosion, carboxylic acid, radiator, high-voltage direct-current transmission

1. INTRODUCTION

A high-voltage direct-current transmission system (HVDC) has the characteristics of a small transmission line size, high transmission efficiency and low power consumption and has therefore become the first choice for excellent resource allocation and long-distance power transmission. The use of a converter valve in HVDC to transform direct current (DC) to alternating current (AC) produces considerable heat [1–2]. Deionized water is typically used as a cooling medium. During HVDC operation,

the electrical conductivity of the cooling water needs to be monitored and maintained below 0.5 μS cm^{-1}. Corrosion of aluminum radiators has been proven to be the main cause of many operation problems, including deposition on graded electrodes and blockage and leakage of cooling water pipes. The main reasons for the corrosion of aluminum radiators are the erosion and corrosion of Al in deionized water, the influence of high voltage, and the action of ions dissolved in deionized water [3–8]. Therefore, the action of ions dissolved in deionized water is considered in this study to determine the law of Al corrosion and provide a theoretical basis for the identification of effective corrosion inhibitors.

Numerous studies have been conducted on using macromolecular organic compounds to protect metallic Al, but there have been relatively few studies on the effect of organic anions on Al corrosion. Organic anions are easily adsorbed at the Al surface because of a large structural volume and charge properties. Therefore, the purpose of this study was to explore the effect of organic anions in solution on Al corrosion to elucidate the specific causes and rules of Al corrosion.

Al corrosion in deionized water containing a prescribed quantity of a short-chain carboxylic acid was investigated in this study. Al corrosion was accelerated by introducing H^+ to clarify the Al corrosion law. The impact of the size of anions produced from organic weak acids on Al corrosion was explored by controlling the length of the carbon chains of carboxylic acids. The Al corrosion law in a series of short-chain carboxylic acid solutions was thus determined, and the organic macromolecular groups were found to effectively alleviate Al corrosion by adsorbing onto the Al surface to form a protective layer.

2. EXPERIMENTAL

2.1 Electrolyte configuration

The electrolytes used in this study were 0.1 mM solutions of formic acid, acetic acid, propionic acid and n-butyric acid. Table 1 shows the pH of the various weak acid solutions at 25 °C.

Table 1. pH of weak acid solutions at 25 °C.

Electrolyte	Ionization constant	pH
HCOOH	1.77×10^{-4}	3.88
CH_3COOH	1.75×10^{-5}	4.38
CH_3CH_2COOH	1.34×10^{-5}	4.44
$CH_3(CH_2)_2COOH$	1.52×10^{-5}	4.41

2.2 Three-electrode system

The test electrochemical system consisted of a working electrode, a reference electrode, a counter electrode and a 0.1 mM saturated monobasic fatty acid electrolyte. A platinum black electrode was used as the counter electrode, and a saturated calomel electrode (SCE) was used as the reference electrode. The SCE potential at 25 °C is 0.228 V (relative to the standard hydrogen electrode (SHE)). The working

electrode was cut from an aluminum radiator. The Al model was 3003, consisting of Si (0.570 wt%), Fe (0.630 wt%), Cu (0.140 wt%), Mn (1.270 wt%), Zn (0.090 wt%), Li (0.030 wt%) and Al (97.310 wt%). Except for a 1-cm^2 working surface, all other parts of Al immersed in solution were coated with epoxy resin. Before testing was performed, the working electrode was polished with emery paper and nanoalumina powder and cleaned by washing with distilled water and anhydrous ethanol; then, the sample was dried in a vacuum drying box.

2.3 Electrochemical tests

The potentiodynamic polarization curve and electrochemical impedance spectra (EIS) were measured using a CHI660D electrochemical workstation.

The potential scanning rate of Al in each electrolyte was 1 mV s^{-1}, and the potential range was 0.800 V (that is, from 0.400 V lower than the stable potential to 0.400 V higher than the stable potential). The corrosion potential and corrosion current density were determined from the polarization curve. The corrosion characteristics of the Al surface were determined from the results of an AC impedance test. The frequency range of the test was 10^{-1}–10^5 Hz, and the amplitude was 5 mV.

In the thermodynamics test, an HH-1 constant-temperature water bath was used to control the solution temperature. The solution temperature was maintained at 25, 35, 45, and 55 °C for 5 days, and the potentiodynamic polarization curves were obtained.

2.4 SEM test

All the samples were prepared for testing by being dried in a vacuum drying box at 30 °C for 12 h to prevent oxidation. SEM was conducted using an SU8010 ultrahigh resolution field emission scanning electron microscope manufactured by Hitachi, Japan.

3. RESULTS AND DISCUSSION

3.1 Electrochemical test

The dominant reaction for Al corrosion in an organic weak acid solution is the hydrogen evolution reaction [9], where the higher the H^+ concentration is, the more positive the potential of the hydrogen evolution reaction is. Figure 1 and Table 2 show that the most positive corrosion potential of Al was measured in the formic acid solution, indicating that the ionization degree of H^+ was highest in the formic acid solution. This result was consistent with the pH test results; as H^+ accelerated Al corrosion, Al exhibited the lowest corrosion resistance in the formic acid solution. After Al was corroded in the different acid solutions for 5 days, the corrosion current density of Al was highest in the formic acid solution and lowest in the n-butyric acid solution, indicating that Al exhibited the highest corrosion resistance in the n-butyric acid solution. Corrosion potential was a criterion for metal corrosion [10], the corrosion current density in the acid solution was higher than that in deionized water, and the corrected

corrosion potential indicated that the presence of H^+ accelerated Al corrosion.

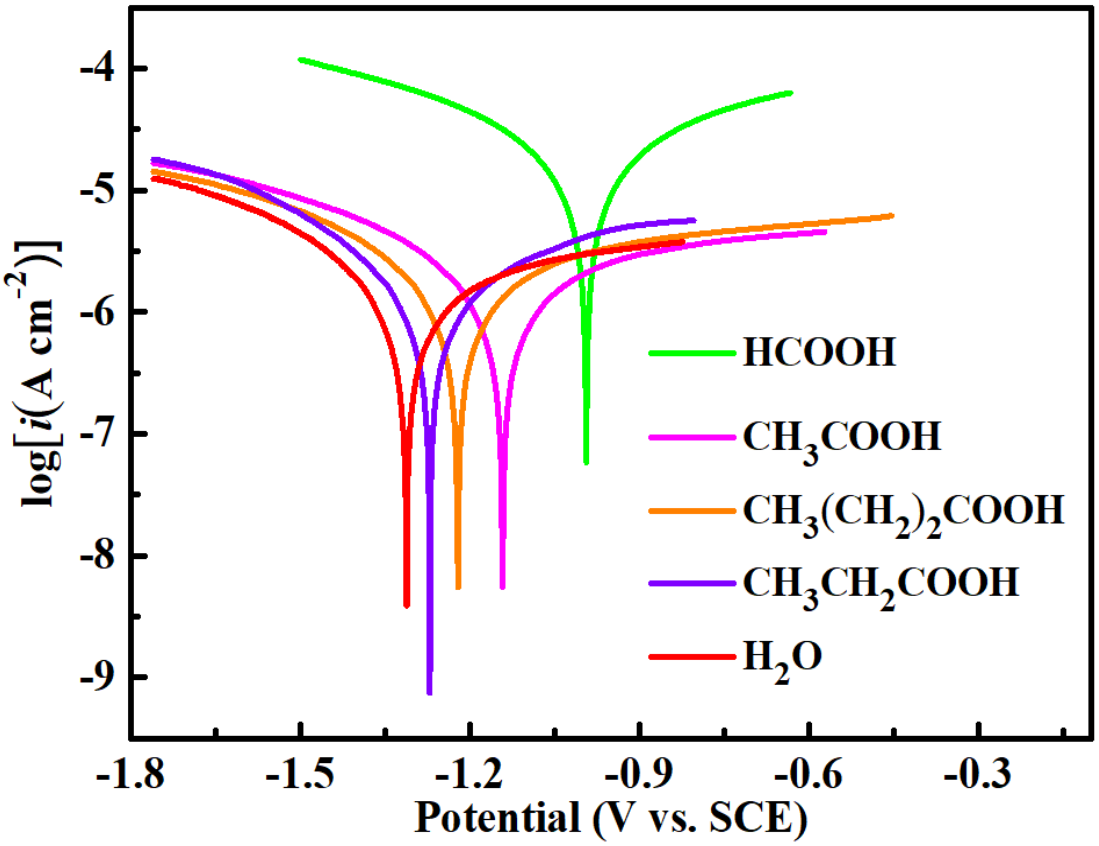

Figure 1. Potentiodynamic polarization curves for Al corrosion in 0.1 mM weak acid solutions at 25 °C for 5 days.

Table 2. Fitted data from polarization curves for Al corrosion in 0.1 mM weak acid solutions at 25 °C for 5 days.

Electrolyte	Corrosion potential E_{corr} (V)	Corrosion current density I_{corr} (μA cm^{-2})
HCOOH	–0.994	9.336
CH_3COOH	–1.141	1.432
CH_3CH_2COOH	–1.257	0.881
$CH_3(CH_2)_2COOH$	–1.222	0.841
H_2O	–1.311	0.796

Note that the pH test results showed a slightly higher H^+ concentration in the n-butyric acid solution than in the propionic acid solution; however, compared to the results obtained in the propionic acid solution, the Al corrosion current density in the n-butyric acid solution was lower and the resistance to the corrosion reaction was higher, indicating that Al had higher corrosion resistance in the n-butyric acid solution, which may have resulted from the n-butyrate ion having a larger volume than the

propionate ion and therefore adsorbing more easily on the surface of alumina film to form a protective layer, thus inhibiting the corrosion of Al. The corrosion of stainless steel by the addition of indole in the cathodic region was effectively alleviated, the organic matter adsorbed on the metal surface by electrostatic interaction could alleviate corrosion, and the adsorption of organic substances in metals and different media was attributed to the size of carbon chains, spatial site resistance effect [11]. Figure 2 shows the EIS curve of the alumina electrode and the equivalent circuit, and Table 3 shows the corresponding parameters obtained by data fitting. R_s represents the solution resistance between the reference electrode (the Luggin capillary mouth) and the Al sheet electrode, C_f represents the capacitance of the oxide film on the Al electrode surface, R_f represents the charge transfer impedance of the solution, C_{dl} represents the electric double layer capacitance of the alumina surface, R_{ct} represents the surface transfer resistance of the Al sheet, and W represents the liquid phase transfer impedance.

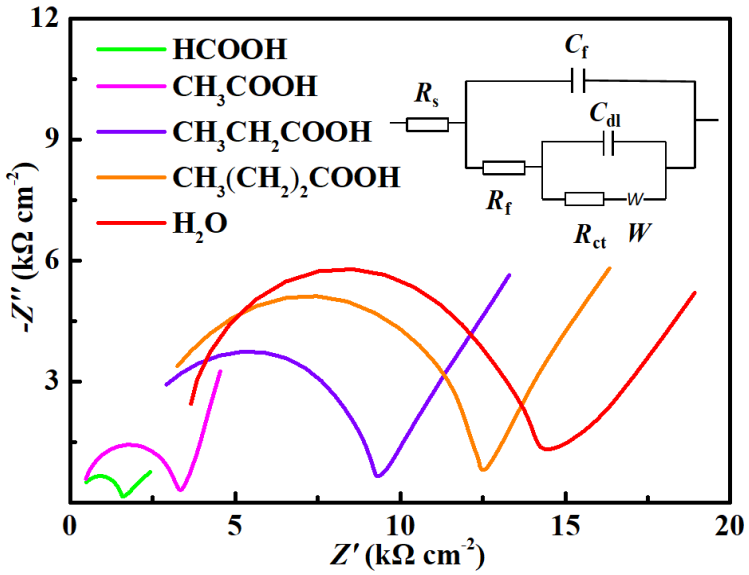

Figure 2. EIS spectra and corresponding equivalent circuit for Al corrosion in 0.1 mM weak acid solutions at 25 °C for 5 days.

Table 3. EIS fitted data for Al corrosion in 0.1 mM weak acid solutions at 25 °C for 5 days.

Electrolyte	R_s (kΩ cm^{-2})	C_f (nF cm^{-2})	R_{ct} (kΩ cm^{-2})	C_{dl} (μF cm^{-2})	R_f (Ω cm^{-2})	W (μΩ cm^{-2})
HCOOH	0.153	89.391	0.596	14.230	7.963	16.050
CH_3COOH	0.345	13.946	2.944	1.926	2.251	10.220
CH_3CH_2COOH	1.619	9.550	7.768	0.901	1.471	13.350
$CH_3(CH_2)_2COOH$	2.032	1.212	10.500	0.823	1.432	12.060
H_2O	3.404	1.102	10.810	0.464	1.521	13.500

R_s is the solution resistance of the electrolyte, and R_{ct} is the charge transfer impedance of the surface of the Al sheet in solution. These parameters reflect the electrolyte conductivity. The solution resistance and charge transfer impedance of the Al electrode were lowest in the formic acid solution,

indicating that the conductivity was largest in the formic acid solution. This result was obtained because formic acid had the largest ionization constant, resulting in the formation of the highest number of ions. The maximum R_s and R_{ct} were obtained in the n-butyric acid solution. This result was obtained because n-butyric acid had the lowest ionization constant and the largest anion, making migration in solution difficult. Therefore, the n-butyric acid solution had the lowest conductivity, resulting in the highest resistance. The oxide film capacitance C_f and the electric double layer capacitance C_{dl} on the surface of the Al sheet were largest in the formic acid solution, and this high capacitance accelerated the corrosion of Al.

3.2 Effect of temperature

In our previous study [4], the reaction between a weak acid and Al was carried out according to the steps of "diffusion → surface adsorption → surface reaction → desorption". As the rate of the reaction of a weak acid and Al depends on the formation rate of the transition product, the activation energy of the Al corrosion reaction is obtained from the Arrhenius equation:

$$i_{corr} = \mathrm{A}\exp\left(\frac{-E_a}{RT}\right) \quad 1)$$

$$\ln i_{corr} = \left(\frac{-E_a}{RT}\right)\left(\frac{1}{T}\right) + \ln \mathrm{A} \quad 2)$$

where i_{corr} is the corrosion current density of the reaction, R is the gas constant (8.314 J mol^{-1} K^{-1}), E_a is the activation energy of the reaction, and T is the temperature (K). A is the electrochemical constant.

The characteristics of the corrosion reaction were analyzed from a thermodynamic perspective. The corrosion reaction was carried out in the different weakly acidic solutions at 25, 35, 45 and 55 °C for 5 days, the potentiodynamic polarization curves were generated, and the corrosion current density at each temperature was fitted. The activation energy E_a was calculated from a plot with $1000/T$ as the abscissa and $\ln i_{corr}$ as the ordinate, and the results are shown in Table 4 and Figure 3.

Table 4. Results from fitting data for Al corrosion in 0.1 mM weak acid solutions for 5 days.

Organic acid	Corrosion current density I_{corr} (μA cm^{-2})				E_a (KJ mol^{-1})
	298.15 K	308.15 K	318.15 K	328.15 K	
HCOOH	9.336	10.230	12.250	13.391	10.401
CH_3COOH	1.432	2.353	3.499	5.020	34.403
CH_3CH_2COOH	0.881	1.707	2.421	4.589	43.432
$CH_3(CH_2)_2COOH$	0.841	1.888	3.996	7.850	61.465

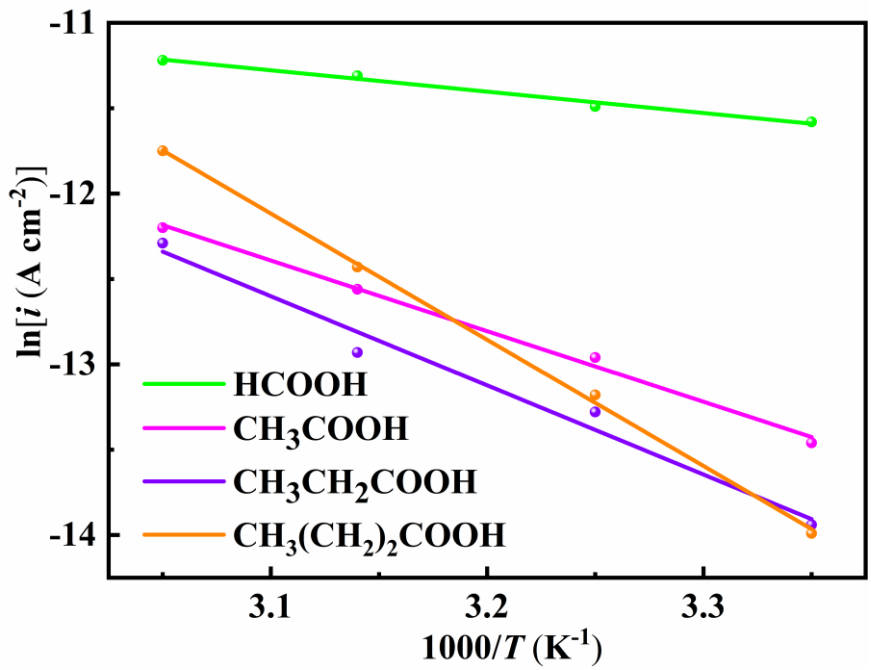

Figure 3. Results for fitting data for Al in various acidic solutions.

The apparent activation energies of Al-22%Si and Al-20%Mg alloys were calculated by the formula, that is the energy barrier between the reactants and the transition state (activated complex), and the corrosion rate increased with the decrease of the apparent activation energy was found [10]. The lowest activation energy was required for the corrosion reaction at the Al electrode in the formic acid solution, indicating that the corrosion reaction occurred most easily and fastest in formic acid, whereas the highest activation energy was required for the corrosion reaction in the n-butyric acid solution, in which the corrosion resistance of the Al electrode was the highest, which was consistent with the electrochemical test results presented above.

3.3 Physical characterization

We conducted SEM to further investigate the corrosion law of the Al electrode surface. The following tests were conducted on an 1 cm × 1 cm Al foil. First, the Al foil was soaked in different weak acid solutions, sealed with fresh-keeping film, and chemically corroded at 25 °C for 5 days. Then, the Al foil was removed, washed with distilled water and anhydrous ethanol, and stored in a sealed bag. The test results are presented below.

The images show that Al corrosion was most severe in the formic acid solution, with clear corrosion pits, whereas Al corrosion in the n-butyric acid solution was barely discernible. This result was obtained because formic acid has a larger ionization constant than n-butyric acid, resulting in a larger number of H^+ at the same acid concentration, which accelerated Al corrosion. This large number of ionized ions in the solution increased the electrical conductivity of the solution, thus increasing the current density of corrosion and accelerating Al corrosion. The ionization constant of n-butyric acid is

small, resulting in the formation of few ions. The organic molecules as corrosion inhibitors would be more easily adsorbed on the metal surface [12, 13]. Compared to formic acid, n-butyric acid has a larger anion radius and occupied more active sites when adsorbed on the surface of Al metal and the oxide film, thereby preventing further contact between H^+ and the oxide film and hindering the progress of the corrosion reaction. These results confirmed the conclusions drawn from the electrochemical tests [14].

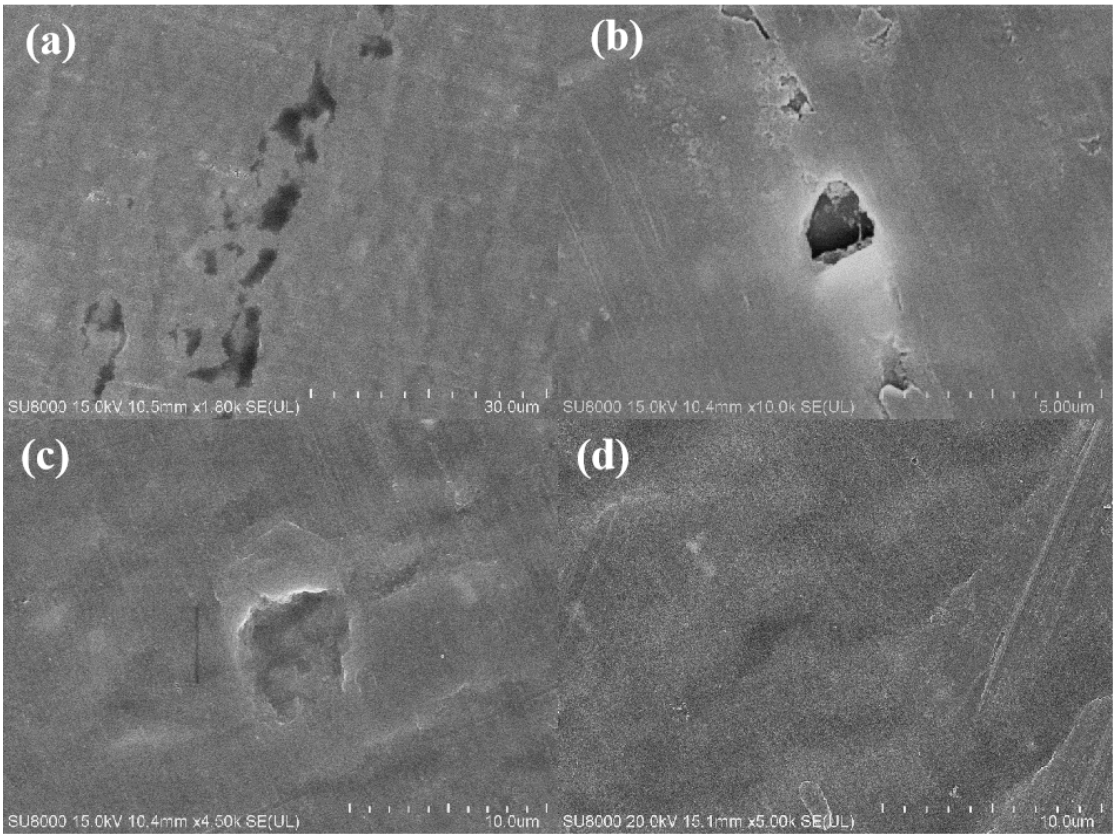

Figure 4. Images of corrosion of Al immersed in HCOOH (a), CH_3COOH (b), CH_3CH_2COOH (c), and C_4H_8O (d) acidic solutions at 25 °C for 5 days.

3.4 Corrosion mechanism analysis

Al typically exhibits passivation behavior in aqueous solution: a firm and dense adhesive passivation oxide film is formed on the Al surface that hinders its corrosion. The oxide film on the surface of a viscous passivation layer is amphoteric and therefore easily dissolved upon exposure of the metal to aggressive acidic and alkaline solutions, resulting in defects in the oxide film through which the H^+ in the solution can further corrode Al. The corrosion products of Al over the pH range of 3.7–4.7 are mainly $Al(OH)_3$. The corrosion reaction of Al in a weakly acidic solution is given below [15–16].

Anodic reaction:

$$Al \longrightarrow Al^{3+} + 3e^- \quad 3)$$

$$Al^{3+} + 3OH^- \longrightarrow Al(OH)_3 \quad 4)$$

Cathodic reaction:

$$O_2 + 2H_2O + 4e^- \longrightarrow 4OH^- \quad 5)$$

$$2H^+ + 2e^- \longrightarrow H_2 \quad 6)$$

In a weakly acidic solution, the large ionization constant of formic acid results in the formation of a large number of H^+ in solution, thereby promoting the cathodic hydrogen evolution reaction and accelerating the corrosion of Al. By comparison, there are fewer H^+ ions in the butyric acid solution, in which the corrosion rate of Al is therefore lower. The corrosion process of Al in aqueous solution includes three steps: dissolution of the Al surface oxide film (hydroxylation), oxidation of the anode metal Al (metallic Al dissolution) and the hydrogen evolution reaction [17–19]. In a weakly acidic solution, the oxide film on the Al surface is usually unstable and gradually dissolves by interacting with the water molecules adsorbed on the surface of the oxide film and H^+ in the solution. Corrosive anions (such as Cl^- and Br^-) typically promote the hydroxylation process at high-energy active sites in the interfacial region. Macromolecular anions (such as n-butyrate) adsorbed by the oxide film occupy a large number of active sites on the surface of the oxide film because of their large ionic radius. The number of active sites occupied by water molecules and hydrogen ions is thereby reduced, which inhibits the hydroxylation process in the solution and the corrosion of Al [20–22].

Figure 5 shows that the corrosion of Al in weakly acidic solutions is a dissolution-precipitation process. At the beginning of corrosion, Al dissolves into the solution in the form of Al^{3+}. Under the mutual attraction of static electricity, Al^{3+} and OH^- in the solution migrate to each other. These ions combine to form an oxide film layer on the electrode surface, that is, insoluble $Al(OH)_3$ is formed and deposited. As the deposition process continues, an oxide film protective layer forms on the electrode surface. The organic anions, water molecules and H^+ in the solution adhere to the surface of the oxide film, among which the corrosive water molecules and H^+ accelerate the dissolution of the oxide film on the Al surface, whereas the organic anions of macromolecules are anti-corrosion groups [23]. These organic anions occupy more active sites on the surface of the oxide film than the water molecules and H^+, thus acting as a protective layer. This behavior can be explained in terms of the large radii of n-butyrate ions, which therefore occupy a large number of active sites when adsorbed on the surface of the oxide film to effectively protect the surface by enabling the formation of a dense oxide film. As a result, the corrosion rate of Al in n-butyric acid solution is the lowest. However, the small volume of formate radicals results in poor protection of the metal oxide film, resulting in a large number of defects in the aluminum oxide film formed in the formic acid solution. Thus, H^+ and water molecules directly contact Al through the oxide film, resulting in the highest corrosion rate of Al in the formic acid solution.

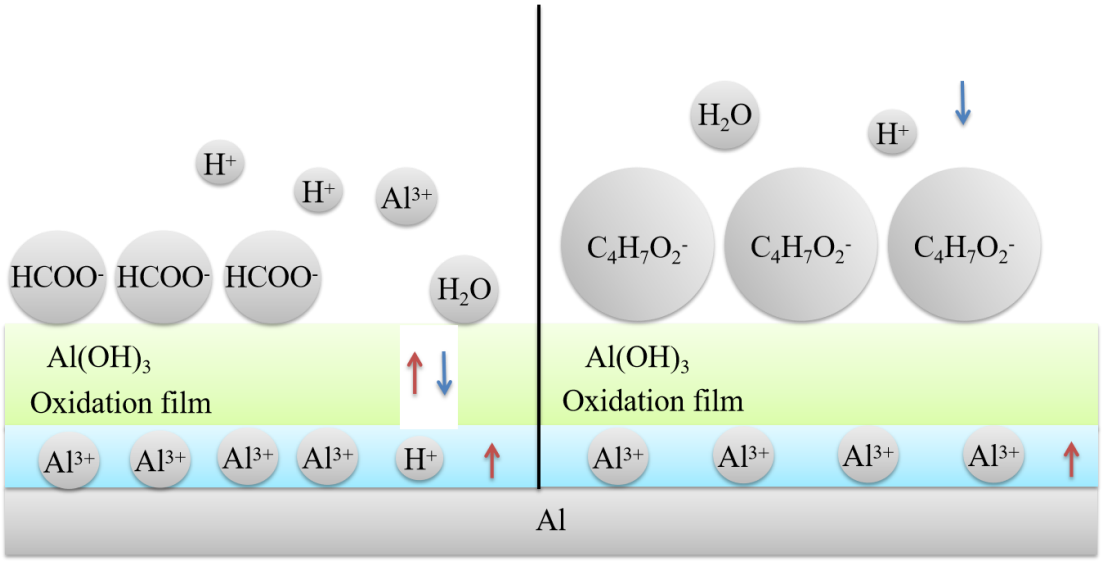

Figure 5. Corrosion mechanism of Al in a weakly acidic solution.

4. CONCLUSIONS

The corrosion law of Al in different short-chain carboxylic acid solutions at 25 °C was investigated in this study. The results showed that the corrosion resistance of Al was lowest in the formic acid solution and highest in the n-butyric acid solution; that is, Al in the n-butyric acid solution exhibited the smallest corrosion current density, the largest charge transfer impedance and the highest corrosion activation energy. These results were obtained because among the weak acids investigated, the ionization constant of formic acid was the largest at the same acid concentration and more H^+ was ionized in the solution, thus accelerating the hydrogen evolution reaction and therefore, the corrosion of Al.

The short-chain carboxylic acid anions in the solution adsorbed onto the oxide film on the metallic Al surface. Among the investigated acids, n-butyrate had the longest carbon chain and largest radius and therefore occupied more active sites on the surface of the oxide film when deposited on the metal oxide film surface; thus, contact between water molecules and hydrogen ions and the oxide film was reduced, and the hydroxylation process in the solution was largely inhibited. The large volume of n-butyric acid radicals also prevented Al^{3+} from leaving the Al base, blocked Al^{3+} diffusion, and inhibited Al corrosion. This discovery provides a theoretical basis for identifying effective corrosion inhibitors.

ACKNOWLEDGEMENTS
This work was supported by the Programs of the China Southern Power Grid (CGYKJXM20210337).

References

1. A. Kalair, N. Abas, N. Khan, *Renew. Sust. Energ. Rev.*, 59 (2016) 1653.
2. Y.H. Qian, Y.Y. Zhou, C.W. Xu, *Adv. Mater. Res,* 354–355 (2011) 1157.
3. Siemens, Thyristor Valves and Associated Eauipment Training Manual, Power Transmission and

Distribution, 2003.
4. P. Zhang, H. Zhang, Y. Xu, H. Li, J. Liu, Y. Fan, S. Wang, *Int. J. Electrochem. Sci.*, 17 (2022) 220324.
5. Y. Tian, H. Li, S. Wang, Y. Fan, *Mater. Corros.*, 72 (2021) 1899.
6. J. Li, L. Hao, F. Zheng, X. Chen, S. Wang,Y. Fan, .*Int. J. Electrochem. Sci.*, 15 (2020) 5320.
7. L. Hao, F. Zheng, X. Chen, J. Li, S. Wang, Y. Fan, *Materials*, 13 (2020) 779.
8. L. Hao, J. Dai, Z. Huang, C. Lei, F. Zheng, J. Li, Y. Fan, S. Wang, *Int. J. Electrochem. Sci.*, 16 (2021) 210529.
9. J. Zhang, W. Wang, *Chem. Afr.*, 3 (2020) 317–321.
10. M. Slimane, F. Kellou-Kerkouche, *Port. Electrochim. Acta*, 38 (2) (2020) 79–98.
11. M. Tussolini, A. Viomar, A.L. Gallina, E. Prado Banczek, M.T. Cunha, P.R.P. Rodrigues, *R. Esc. Minas, Ouro Preto*, 66 (2) (2013) 215–220.
12. I.O. Arukalam, I.C. Madufor, O. Ogbobe, E.E. Oguzie, *Pigment. Resin Technol.*, 43 (3) (2014) 151–158.
13. A.S. Patel, V.A. Panchal, N.K. Shah, *Bull. Mater. Sci.*, 35 (2) (2012) 283–290.
14. P. Jinturkar, Y.C. Guan, K.N. Han, *Corrosion*, 54 (2) (1998) 106.
15. J. Zhang, M. Klasky, B.C. Letellier, *J. Nucl. Mater.*, 384 (2) (2009) 175.
16. E. McCafferty, *Corros. Sci.*, 45 (7) (2003) 1421.
17. I. Weber, B. Mallick, M. Schild, S. Kareth, R. Puchta, R. Eldik, *Chem. Eur. J.*, 20 (38) (2014) 12091.
18. J. Wysocka, S. Krakowiak, J. Ryl, K. Darowicki, *J. Electroanal. Chem.*, 778 (2016) 126.
19. T. Nishimura, T. Kodama, *Corros. Sci.*, 45 (5) (2003) 1073.
20. M. Lashgari, E. Kianpour, E. Mohammadi, *J. Mater. Eng. Perform*., 22 (2013) 3620.
21. M. Lashgari, *Electrochim. Acta*, 56 (9) (2011) 3322.
22. D. Susac, X. Sun, R.Y. Li, P.C. Wong, K.A.R. Mitchell, R. Champaneria, *Appl. Surf. Sci.*, 239 (1) (2004) 45.
23. W. Zhang, P. Li, H. Xu, R. Sun, P. Qing, Y. Zhang, *J. Hazard. Mater*., 268 (2014) 273.